J. Mod. Trends Math. Sci., 1 (2025), 1–13

Online: ISSN 2008-949X

JOURNAL OF MODERN TRENDS IN MATHEMATICAL SCIENCES
JMTMS

Impact of Rastall Gravity on PSR J0348+0432 Hybrid Star with Strange Quark Matter

Sunaiha Naeem[a], Arfa Waseem[a,*]

[a]*Department of Mathematics, Government College Women University, Sialkot, Pakistan.*

Abstract

This paper presents a systematic theoretical investigation of isotropic compact star within the framework of Rastall gravity, emphasizing the influence of Rastall parameter on the stability and physical properties of compact stellar model PSR J0348+0432. A static and spherically symmetric spacetime filled with a perfect fluid is considered, and the interior geometry of the compact star is described using the Durgapal-Fuloria metric function. The stellar matter distribution is modeled as a two component system consisting of normal baryonic matter and strange quark matter, where the quark phase is governed by the MIT bag model equation of state. The unknown parameters of the model are determined by applying standard junction conditions, matching the interior solution with the observed masses and radii of selected compact stellar candidates. The physical viability of the obtained solutions is examined through a detailed analysis of matter variables, energy conditions, equation of state behavior, mass function, and causality condition for different values of the Rastall parameter. The results confirm that the resulting stellar configurations remain stable, well behaved, and physically acceptable within Rastall gravity, supporting its effectiveness as an alternative framework for modeling realistic compact stars.

Keywords: Rastall theory, Compact stars, Durgapal-Fuloria metric, MIT Bag model, Stability analysis.

2020 MSC: 83C15, 83D05, 85A20, 76E20.

1. Introduction

The search for consistent extensions of Einstein's general theory of relativity (GTR) has inspired a wealth of alternative gravitational frameworks. Among various alternative approaches, Rastall theory (henceforth $\mathcal{RT}$) has emerged as a particularly intriguing and distinctive formulation [26, 27]. By relinquishing the conventional postulate of strict energy-momentum conservation, black hole allows for a non vanishing divergence of the energy momentum tensor (EMT) in curved spacetime, thereby instituting a non minimal coupling between matter and geometry. This coupling redefines the classical correspondence between gravitational curvature and the distribution of energy. This departure has been the subject of sustained criticism as scholars argue that the apparent non conservation of EMT represents a serious deviation from the principles of classical physics. Also, some researchers contend that this deviation can be viewed as a natural consequence of spacetime curvature or as an indication of net energy creation in certain physical systems [27, 39, 9, 14, 15]. Further debate has arisen due to the absence of a

*Corresponding author
Email addresses: sunaihanaeem.19@gmail.com (Sunaiha Naeem), arfa.waseem@gcwus.edu.pk (Arfa Waseem)

doi: 10.22436/...

Received: December 01, 2025 Revised: December 03, 2025 Accepted: December 15, 2025

fully formulated Lagrangian representation for $\mathcal{RT}$, prompting questions regarding the theory's internal consistency and completeness. This is particularly in contrast with the rigorous variational formulations underlying GTR. Despite these conceptual challenges, the theoretical versatility and predictive capacity of the framework are evident across a broad range of applications. Its parametrized deviation from classical theory facilitates the construction of novel spherically symmetric stellar models [21], enabling detailed investigations into the equilibrium, stability and internal structure of compact objects under extreme conditions. Beyond isotropic configurations, $\mathcal{RT}$ has been successfully employed to model the isotropization and complexity reduction of matter distributions [22, 23]. Sohail et al. [37] investigated anisotropic compact stellar structures in modified Rastall teleparallel gravity using minimal geometric deformation and verified equilibrium and stability. The stability analyses of anisotropic stellar structures using the cracking method [19] have further demonstrated the robustness of this theory in describing realistic astrophysical systems. Das et al. [10] analyzed charged anisotropic strange star models in $\mathcal{RT}$ using the MIT bag model and confirmed stability and physical viability. Additionally, the implementation of Durgapal-Lake solutions within this framework has allowed for a systematic exploration of compact stellar configurations, revealing subtle dependencies of physical properties on the non-minimal coupling parameter [44, 42, 43]. A growing number of investigations emphasize the sustained significance of $\mathcal{RT}$ as studies have examined its role in compact object modeling and in clarifying the connection between matter and geometry [35, 38, 34, 40, 41, 29, 32, 4]. Mustafa et al. [20] studied anisotropic compact stellar models in Rastall gravity and confirmed their physical acceptability and stability under observational constraints. These investigations establish $\mathcal{RG}$ as a versatile and empirically significant paradigm that sustains theoretical innovation and supports observational progress in modern astrophysics and cosmology.

Alongside the gravitational modifications introduced by $\mathcal{RT}$, the composition of matter within compact stars plays a crucial role in determining their physical behavior. Strange quark matter is widely regarded as a prime candidate for the most stable form of baryonic matter, composed of deconfined up, down, and strange quarks under extreme density conditions. Itoh [18] first suggested that if baryons are made of fundamental constituents, these particles may exist freely in the interiors of ultra-dense stars, giving rise to quark or hybrid star configurations. At sufficiently high densities and temperatures, quarks behave almost independently due to asymptotic freedom [12]. Witten [45] proposed that strange matter can form either via a quark–hadron phase transition in the early universe or through the conversion of neutron stars at ultrahigh densities. Cheng et al. [7] described the realistic strange quark matter in beta equilibrium as an almost equal mixture of up, down, and strange quarks, with a slight under-abundance of the strange component. Bodmer [2] argued that at densities exceeding nuclear thresholds, a transition from hadronic to strange quark matter could occur during supernova explosions, making it a viable constituent of neutron star cores. In addition, quark matter has been applied in galactic contexts. Rahaman et al. [25] demonstrated that modeling the galactic halo with quark matter produces a gravitationally attractive spacetime consistent with observed flat rotation curves. More recent studies have further explored strange quark stars in various modified gravity frameworks and higher-dimensional scenarios, highlighting their structural properties and mass–radius relations [8, 13, 17, 24, 31, 36].

Extending this line of inquiry, refined metric constructions have proven indispensable in capturing the delicate gravitational architecture that governs compact stellar systems. Among them, the Durgapal-Fuloria solution [11] holds a distinguished place. The mathematical consistency of this model adherence to basic physical constraints. The adaptability to diverse matter distributions make this model particularly suited for the study of dense relativistic objects. This framework has therefore been employed in different gravitational scenarios to investigate stability and dynamical behavior [28, 30, 33]. Understanding the internal structure and stability of compact stellar objects requires the realistic modeling of both their geometry and matter composition. This work analyzes the isotropic stellar configurations using a two-fluid model that incorporates ordinary baryonic matter alongside strange quark matter. Section **2** derives the interior solutions of the field equations for this model, while Sect. **3** employs a well-behaved metric to describe the stellar interior. In Sect. **4**, boundary conditions are applied, and the physical viability of the models is examined through causality, energy conditions, and mass–radius relations. Finally, Sect. **5**

summarizes the main results and highlights their significance for hybrid star configurations in modified gravity.

2. Interior Solution in Rastall Gravity with Two-Fluid Isotropic Model

In the framework of classical GTR, the EMT $T_{\alpha\beta}$ is postulated to obey the conservation condition

$$\nabla_\beta T^\beta_\alpha = 0, \tag{1}$$

ensuring precise local conservation of energy and momentum. Rastall [26] proposed a compelling generalization of this fundamental principle, wherein the divergence of the EMT is directly coupled to the derivative of the Ricci scalar. This extension gives rise to a generalized gravitational formalism, elegantly expressed as

$$\nabla_\beta T^\beta_\alpha = J_\alpha, \tag{2}$$

where J_α vanishes in flat spacetime but assumes non-zero values in the presence of curvature. Specifically, one may define

$$J_\alpha = \Phi\, \partial_\alpha \mathcal{R}, \quad \mathcal{R} = g^{\alpha\beta}\mathcal{R}_{\alpha\beta}, \tag{3}$$

with Φ representing a constant coupling parameter. Accordingly, the field equations within $\mathcal{RT}$ are formulated as

$$\mathcal{R}_{\alpha\beta} - \frac{1}{2}g_{\alpha\beta}\mathcal{R} + \kappa\Phi g_{\alpha\beta}\mathcal{R} = \kappa T_{\alpha\beta}, \tag{4}$$

where κ denotes the gravitational coupling constant. Introducing the dimensionless Rastall parameter $\Phi = \kappa\Phi$, the field equations become

$$G_{\alpha\beta} + \Phi g_{\alpha\beta}\mathcal{R} = \kappa\frac{4\Phi - 1}{6\Phi - 1}T_{\alpha\beta}. \tag{5}$$

It is noteworthy that the parameter values $\Phi = 1/4$ and $\Phi = 1/6$ are inadmissible, as they induce singularities within the governing equations. To investigate a static, spherically symmetric interior configuration, the line element is considered as

$$ds^2 = -e^{\nu(r)}dt^2 + e^{\mu(r)}dr^2 + r^2 d\theta^2 + r^2\sin^2\theta d\phi^2, \tag{6}$$

where $\nu(r)$ and $\mu(r)$ are functions of the radial coordinate r. The matter distribution is modeled as a two-fluid system with isotropic pressure, characterized by the effective EMT

$$T^0_0 = \rho^{Ras}_{eff} = \rho^{Ras} + \rho^{Ras}_q, \quad T^1_1 = T^2_2 = T^3_3 = -(p^{Ras} + p^{Ras}_q), \tag{7}$$

where ρ^{Ras} represents the conventional matter energy density, ρ^{Ras}_q accounts for the contribution from the secondary fluid, and p and p_q denote their respective isotropic pressures. Consequently, the total effective pressure is $p_{eff} = p + p_q$.

Within this setup, the Rastall modified field equations governing the interior geometry are expressed as:

$$8\pi\left(\frac{4\Phi-1}{6\Phi-1}\right)(\rho^{Ras}+\rho^{Ras}_q) = \frac{1-e^{-\mu}}{r^2} + \frac{\mu'}{r}e^{-\mu} + \Phi e^{-\mu}\Big(\nu'' + (\nu')^2 + \nu'\mu' - \frac{2}{r}(\mu'-\nu') - \frac{2(e^\mu-1)}{r^2}\Big), \tag{8}$$

$$8\pi\left(\frac{4\Phi-1}{6\Phi-1}\right)(p^{Ras}+p^{Ras}_q) = -\frac{1-e^{-\mu}}{r^2} + \frac{\nu'}{r}e^{-\mu} - \Phi e^{-\mu}\Big(\nu'' + (\nu')^2 + \nu'\mu' - \frac{2}{r}(\mu'-\nu') - \frac{2(e^\mu-1)}{r^2}\Big), \tag{9}$$

$$8\pi\left(\frac{4\Phi-1}{6\Phi-1}\right)(p^{Ras}+p^{Ras}_q) = \frac{e^{-\mu}}{4}\left(2\nu'' + (\nu')^2 + \frac{4\nu'}{r} - \frac{2\mu'}{r} - \nu'\mu'\right) - \Phi e^{-\mu}\Big(\nu'' + (\nu')^2 + \nu'\mu' - \frac{2}{r}(\mu'-\nu') - \frac{2(e^\mu-1)}{r^2}\Big). \tag{10}$$

The thermodynamic behavior of quark matter within the stellar interior is modeled through the MIT bag equation of state (EoS), which establishes a linear relationship between pressure and energy density, expressed as

$$p_q^{Ras} = \frac{1}{3}(\rho_q^{Ras} - 4\mathcal{B}_g), \tag{11}$$

where $(\mathcal{B}_g)$ denotes the bag constant, encapsulating the energy difference between the perturbative and non-perturbative vacua of quantum chromodynamics. This parameter is a fundamental characteristic of quark confinement and serves to quantify the intrinsic vacuum pressure resisting de-confinement. For the conventional baryonic matter, we adopt a barotropic form for the pressure, assuming direct proportionality with the corresponding energy density:

$$p^{Ras} = m\rho^{Ras}, \tag{12}$$

where m is the dimensionless parameter constrained within the physically admissible range $(0 < m < 1)$, explicitly excluding $(m = \frac{1}{3})$ to avoid degeneracy with radiation-like behavior.

3. Durgapal-Fuloria Spacetime

In order to obtain an exact interior configuration within the adopted gravitational framework, we employ the Durgapal-Fuloria [11] metric potential, a well-known ansatz frequently utilized in modeling relativistic stellar interiors owing to its regular behavior and analytic conformity. Within this scheme, we adopt the following forms for the temporal and radial metric components

$$e^{\mu(r)} = \frac{7(1+Ar^2)^2}{7-Ar^2(10+Ar^2)}, \quad e^{\nu(r)} = B(1+Ar^2)^4, \tag{13}$$

where A and B are constants to be determined from the boundary and physical conditions. Incorporation of Eq. (13) into the governing equations (8)–(12) allows the determination of the matter density and pressure of the stellar configuration. Accordingly, the energy density and pressure of the ordinary matter and quark matter are given by

$$\begin{aligned}\rho(r)^{Ras} &= \frac{28\mathcal{B}_g}{7(-1+3m)} + \frac{1}{\pi(1+Ar^2)^4(-1+4\Phi)}\Big(A(-1+6\Phi)\Big(3-12\Phi+ \\ &\quad Ar^2(-41-236\Phi+Ar^2(-51+460\Phi+Ar^2(-7+44\Phi)))\Big)\Big), \end{aligned}\tag{14}$$

$$\begin{aligned}p(r)^{Ras} &= \frac{m}{7(-1+3m)(\pi(1+Ar^2)^4(-1+4\Phi))}\Big(A(-1+6\Phi)\Big(3-12\Phi+ \\ &\quad Ar^2(-41-236\Phi+Ar^2(-51+460\Phi+Ar^2(-7+44\Phi)))\Big)\Big) \\ &\quad + \frac{28m\mathcal{B}_g}{7(-1+3m)}, \end{aligned}\tag{15}$$

$$\rho_q^{Ras}(r) = \frac{-1}{7(-1+3m)(\pi(1+Ar^2)^4(-1+4\Phi))}\Bigg(A(-1+6\Phi)(-(1+Ar^2) (-4+9m+2A(7+m)r^2+A^2(2+m)r^4)+(1+m)(-3+ Ar^2(-59+Ar^2(115+11Ar^2)))\Phi)\Bigg)+\frac{28\mathcal{B}_g}{7(-1+3m)}, \tag{16}$$

$$p_q^{Ras}(r) = \frac{-1}{7(-1+3m)(\pi(1+Ar^2)^4(-1+4\Phi))}\Bigg(3A(-1+6\Phi)(-(1+Ar^2) (-4+9m+2A(7+m)r^2+A^2(2+m)r^4)+(1+m)(-3+ Ar^2(-59+Ar^2(115+11Ar^2)))\Phi)\Bigg)+\frac{28m\mathcal{B}_g}{7(-1+3m)}. \tag{17}$$

4. Interface Matching and Stellar Structure

To investigate the geometry and distinctive attributes of celestial entities, a seamless link among the interior and external geometries of celestial objects is required. Using this technique, the Schwarzschild geometry is considered, given by

$$ds_+^2 = -\left(1-\frac{2\mathcal{M}}{r}\right)dt^2+\left(1-\frac{2\mathcal{M}}{r}\right)^{-1}dr^2+r^2(d\theta^2+\sin^2\theta d\phi^2), \tag{18}$$

where $\mathcal{M}$ indicates the star's internal total mass. The functions g_{tt} and g_{rr} are continuous at $r=\mathcal{R}$, providing

$$1-\frac{2\mathcal{M}}{\mathcal{R}} = B(1+A\mathcal{R}^2)^4, \tag{19}$$

$$\left(1-\frac{2\mathcal{M}}{\mathcal{R}}\right)^{-1} = \frac{7(1+A\mathcal{R}^2)2}{7-A\mathcal{R}^2(10+A\mathcal{R}^2)}, \tag{20}$$

Equations (10) and (11) may be adopted to assess the parameters (A, B) corresponding to the radius and mass, resulting in

$$A = \frac{7\mathcal{M}}{-7\mathcal{M}\mathcal{R}^2+6\mathcal{R}^3+2\sqrt{\mathcal{R}^5(-14\mathcal{M}+9\mathcal{R})}}, \tag{21}$$

$$B = \frac{-2\mathcal{M}+\mathcal{R}}{\mathcal{R}(1+A\mathcal{R}^2)^4}. \tag{22}$$

Moreover, the bag constant $\mathcal{B}_g$ follows directly from the requirement that the radial pressure must vanish at the stellar boundary. Imposing the condition ($p(\mathcal{R})=0$) on the pressure profile yields the closed form expression for bag constant given below.

$$\mathcal{B}_g = -\frac{A(-1+6\Phi)}{28\pi(1+AR^2)^4(-1+4\Phi)}\Big(3-12\Phi+AR^2(-41-236\Phi + AR^2(-51+460\Phi+AR^2(-7+44\Phi)))\Big). \tag{23}$$

To represent our model graphically, it is essential to select reasonable values for the parameters A and B. For this purpose, we determine the values of A and B by considering the strange star PSRJ0348 + 0432, which has an estimated radius $R = 10.29^{+1.01}_{-0.86}$ km and a mass $M = 1.44^{+0.06}_{-0.07}\ M_\odot$.

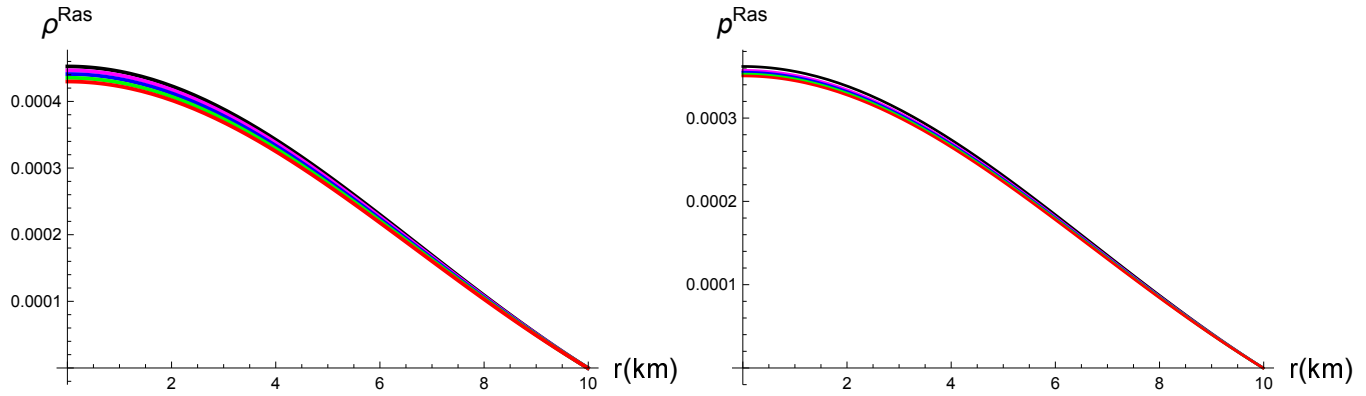

Figure 1: Energy density and pressure with $\Phi = 0$ (black), $\Phi = 0.0021$ (Magenta), $\Phi = 0.0041$ (blue), $\Phi = 0.0061$ (Green), and $\Phi = 0.0081$ (Red).

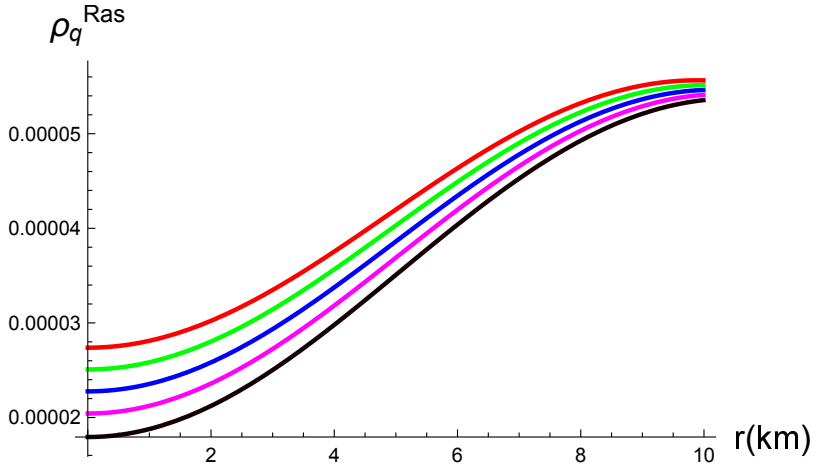

Figure 2: Quark energy density with $\Phi = 0$ (black), $\Phi = 0.0021$ (Magenta), $\Phi = 0.0041$ (blue), $\Phi = 0.0061$ (Green), and $\Phi = 0.0081$ (Red).

4.1. Significance of Matter Constituents in Stellar Modeling

Whenever investigating celestial models, it is crucial to understand that compact entities exhibit higher matter density and pressure inside their celestial formations. Figure **1** depicts energy density and pressure variations for different values of Rastall parameter. Moreover, the profile of matter density corresponding to the quark matter is shown in Fig. **2**. The figure shows that quark density is positive inside the fluid sphere.The Durgapal-Fuloria assumption with $\Phi = 0$ is used in these representations to show the typical GR findings. At the star's core, precisely at $r = 0$, the restrictions for maximum density and pressure are stated as:

$$\frac{d\rho^{Ras}}{dr} = 0, \quad \frac{dp^{Ras}}{dr} = 0, \quad \frac{d^2\rho^{Ras}}{dr^2} < 0, \quad \frac{d^2p^{Ras}}{dr^2} < 0. \tag{24}$$

Figure **3** demonstrates how matter components vary between star candidates with different Rastall parameter values. Notably, pressure and energy density are most intense at the star's center and decrease as one moves outwards in the stellar model. This steady decline underlines the presence of thick and compact cores, with pressures approaching zero at the stellar edge. The juxtaposition of the pressure and concentration of energy values with the maximality constraints given in Eq. (24) confirm the formally reasonable and cohesive state of the matter components under this assumption.

4.2. Constraints on Energy Distribution

Energy constraints are crucial for characterizing the emergence and arrangement of matter. These limits help differentiate conventional from unusual matter distributions within stellar structures and serve to

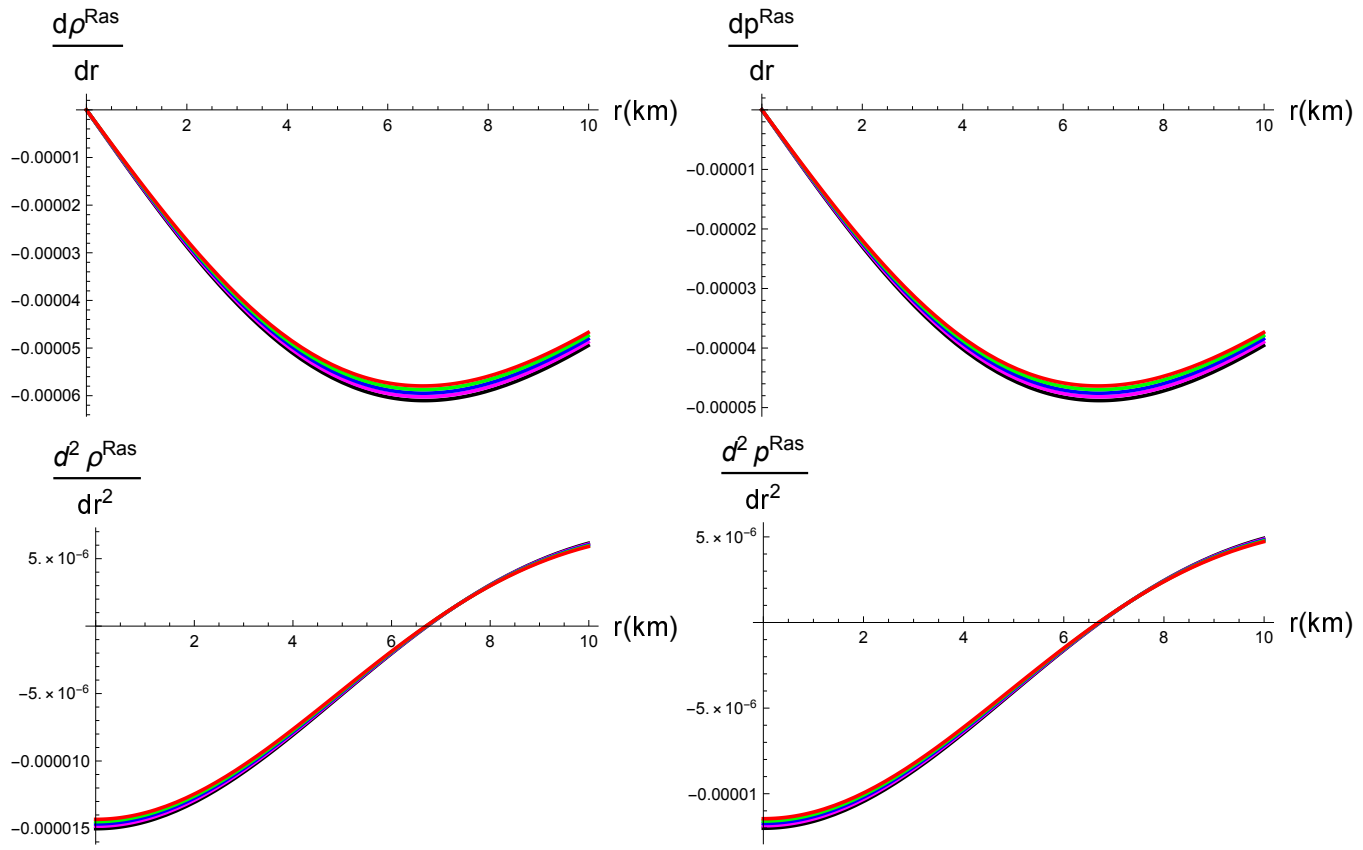

Figure 3: Differential form of density and pressure with $\Phi = 0$ (black), $\Phi = 0.0021$ (Magenta), $\Phi = 0.0041$ (blue), $\Phi = 0.0061$ (Green), and $\Phi = 0.0081$ (Red).

verify the consistency of the proposed theoretical model. Within the context of $\mathcal{RT}$, for a fluid configuration exhibiting isotropy, these constraints can be expressed as:

- Null : $\rho^{Ras} + p^{Ras} \geqslant 0$,
- Weak: $\rho^{Ras} \geqslant 0, \quad \rho^{Ras} + p^{Ras} \geqslant 0$,
- Strong: $\rho^{Ras} + 3p^{Ras} \geqslant 0$,
- Dominant: $\rho^{Ras} - p^{Ras} \geqslant 0$.

The behavior of energy conditions illustrated in Fig. **4** demonstrates that all conditions are satisfied, implying that the stellar configuration consists of standard matter. The satisfaction of these conditions further reinforces the physical consistency of the Rastall framework.

4.3. Characterization via Equation of State

The EoS provides a fundamental framework for describing the thermodynamic behavior of matter under prescribed physical conditions. The EoS parameter represents a dimensionless measure that quantifies the correspondence between internal pressure and energy density. In the context of $\mathcal{RT}$, this parameter can be formulated from Eqs. (8) and (9) as

$$\omega^{Ras} = \frac{p^{Ras}}{\rho^{Ras}}.$$

Figure **5** depicts the variation of ω^{Ras} for a selection of compact stellar objects. The analysis demonstrates that ω^{Ras} consistently lies between 0 and 1, indicating the presence of conventional, non-exotic matter within these highly dense configurations.

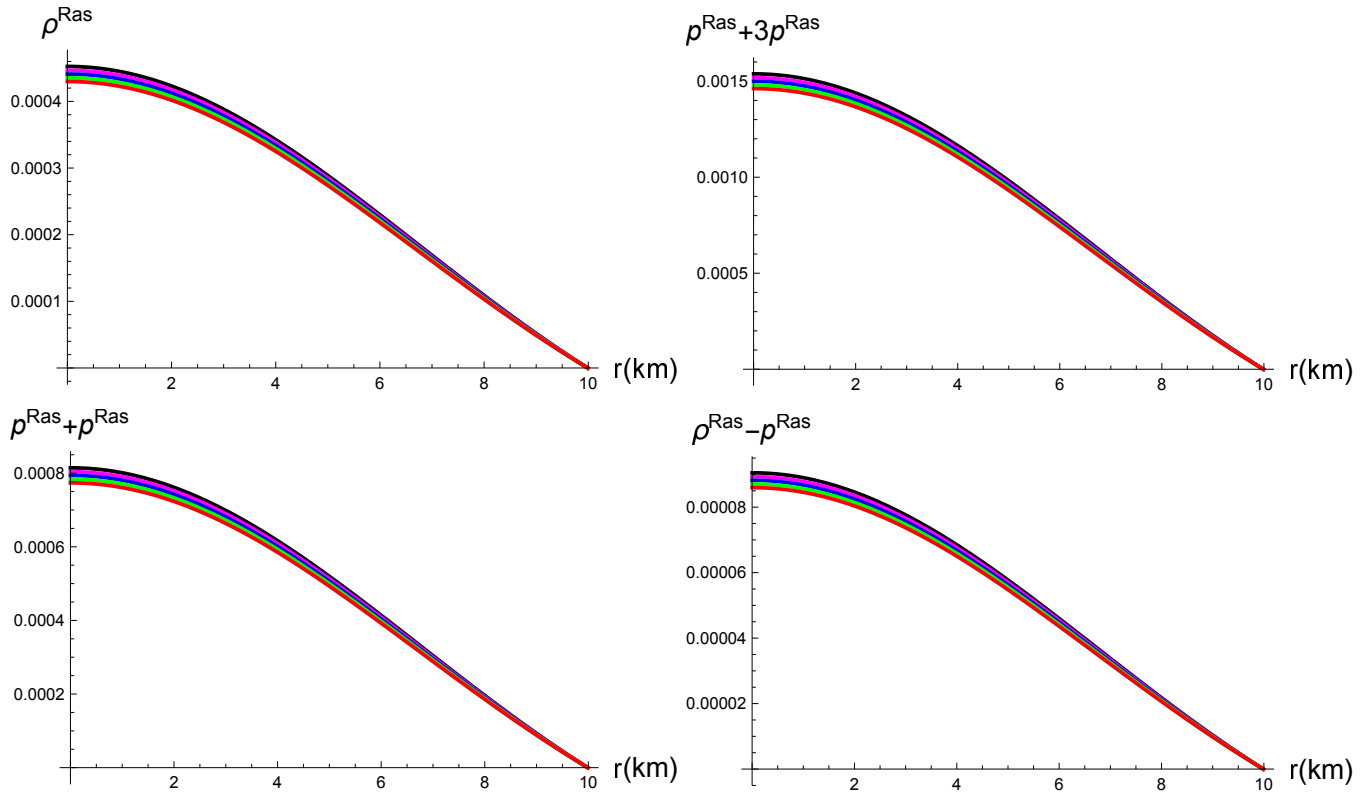

Figure 4: Illustration of energy distributions with $\Phi = 0$ (black), $\Phi = 0.0021$ (Magenta), $\Phi = 0.0041$ (blue), $\Phi = 0.0061$ (Green), and $\Phi = 0.0081$ (Red).

4.4. Compactness and Surface Redshift of Star

Following the work of Buchdahl [3], a spherically symmetric object with isotropic pressure is subject to an upper limit on its mass-to-radius ratio, satisfying $\frac{\mathcal{M}}{\mathcal{R}} < \frac{4}{9}$. For the present model, the gravitational mass corresponding to a given radius can be expressed as:

$$\mathcal{M}^{Ras} = 4\pi \int_0^{\mathcal{R}} r^2 \rho_{eff}^{Ras} \, dr.$$

The ratio of mass to radius, often referred to as the compactness parameter, is defined by

$$u^{Ras} = \frac{\mathcal{M}^{Ras}}{\mathcal{R}}.$$

The surface gravitational redshift (z_s) plays a crucial role in revealing the correlation between the stellar constituents and the equation of state. When expressed in terms of compactness, the gravitational redshift takes the form:

$$z_s^{Ras} = \frac{1}{\sqrt{1-2u^{Ras}}} - 1.$$

The distributions of mass, compactness, and gravitational redshift are depicted in Figure **5**. It is apparent that the mass begins at zero at the center and grows steadily toward the stellar boundary, demonstrating a regular and stable internal structure. The compactness curve adheres to the upper Buchdahl limit ($\frac{\mathcal{M}}{\mathcal{R}} < \frac{4}{9}$), and the redshift values lie within the expected bounds for isotropic configurations ($z_s \leqslant 2$) [3, 1].

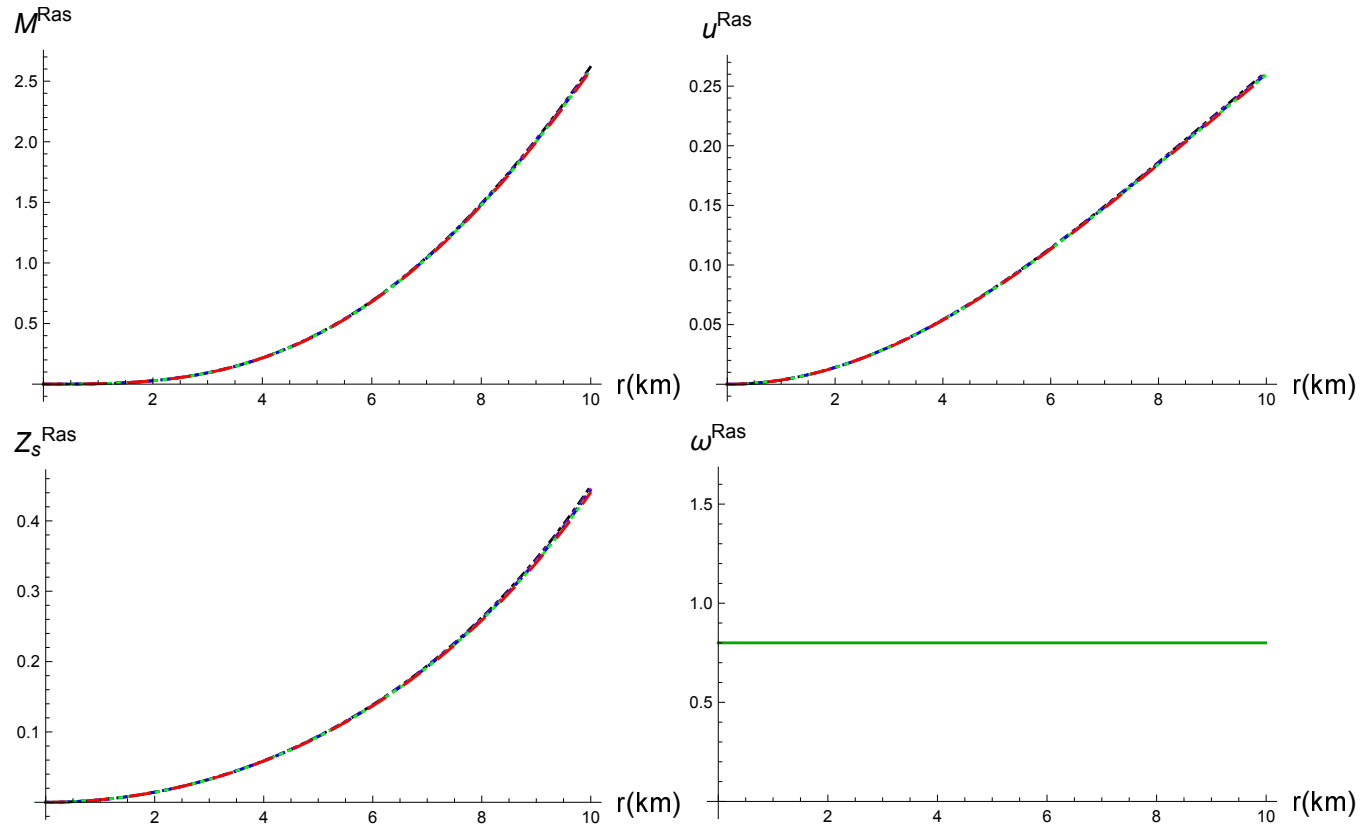

Figure 5: Role of mass, compactness, and redshift with $\Phi = 0$ (black), $\Phi = 0.0021$ (Magenta), $\Phi = 0.0041$ (blue), $\Phi = 0.0061$ (Green), and $\Phi = 0.0081$ (Red).

4.5. Stability Analysis of Stellar Configurations

The physical plausibility of astrophysical models can be rigorously evaluated through their response to external perturbations. Structural stability constitutes a fundamental criterion for the acceptability and realism of any proposed stellar model. To investigate the stability of the selected compact objects, several diagnostic measures are employed, including the speed of sound and the adiabatic index. These parameters offer critical insights into the internal behavior of the configuration under varying conditions, allowing a comprehensive assessment of its robustness and physical reliability. The square of the sound

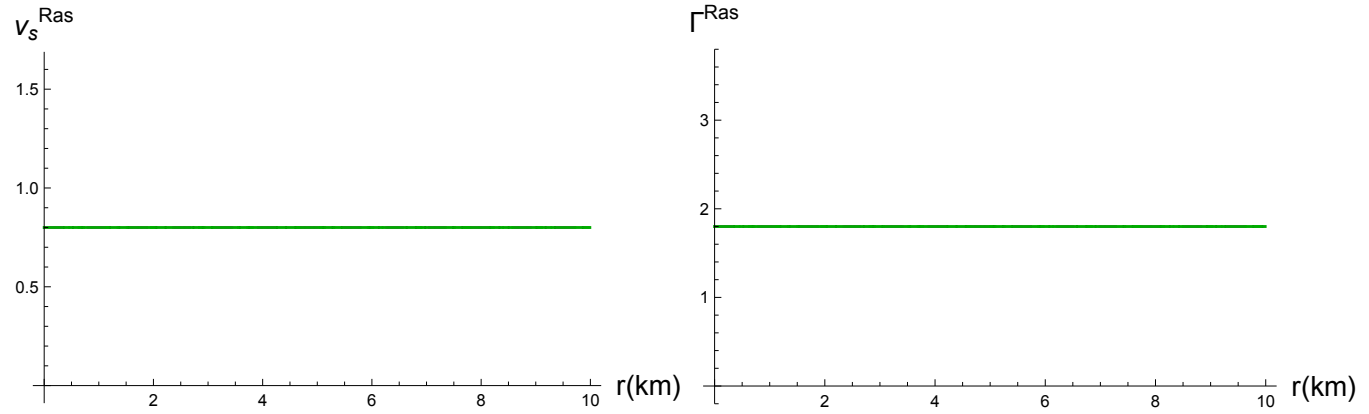

Figure 6: Role of square speed of sound and adiabatic index with $\Phi = 0$ (black), $\Phi = 0.0021$ (Magenta), $\Phi = 0.0041$ (blue), $\Phi = 0.0061$ (Green) and $\Phi = 0.0081$ (Red).

speed, defined as

$$v_s^2 = \frac{dp^{Ras}}{d\rho^{Ras}},$$

must remain within the causal bounds $0 \leqslant v_s^2 \leqslant 1$ to ensure a stable stellar structure [16]. In addition, the adiabatic index serves as a key indicator of dynamical stability [5, 6], which for isotropic matter distributions is given by

$$\Gamma = \frac{\rho^{Ras} + p^{Ras}}{p^{Ras}} \frac{dp^{Ras}}{d\rho^{Ras}}.$$

Within the relativistic framework, a configuration is considered dynamically stable if the adiabatic index satisfies $\Gamma > 4/3$ [30].

Figure **6** demonstrates that examined star comply with both causality constraints and the adiabatic stability criterion for selected values of the parameter Φ. Consequently, the compact objects display coherent and physically consistent behavior in accordance with the Durgapal-Fuloria ansatz within the framework of Rastall gravity.

Table 1: Comparison of key physical quantities in GTR and $\mathcal{RT}$.

Physical Quantity	$\Phi = 0$ (GTR)	$\Phi = 0.0061$
Central density ρ_c^{Ras} (gm/cm^3)	6.08637×10^{14}	5.8575×10^{14}
Central quark density ρ_{qc}^{Ras} (gm/cm^3)	2.41331×10^{13}	3.37435×10^{13}
Central pressure p_c^{Ras} (dyne/cm^2)	4.37606×10^{35}	4.2115×10^{35}
Mass (km)	2.61429	2.57765
Compactness	0.2615	0.2579

5. Conclusions

In this study, we explored the physical characteristics of compact stellar objects within the framework of $\mathcal{RT}$, employing the Durgapal–Fuloria ansatz to construct a viable interior solution. By examining the physical behavior, matter distribution, stability criteria, and gravitational attributes of the considered stars, we demonstrated that the proposed model aligns well with fundamental physical requirements and offers an internally consistent description of dense astrophysical systems.

The analysis is supported by a detailed investigation of the energy density, pressures and related physical indicators for several chosen values of the Rastall parameter. The graphical interpretations provided throughout the work highlight the influence of modified gravity on stellar structure and confirm the credibility of the obtained solutions.

To consolidate the findings, the main outcomes of the paper are summarized below:

- **Matter Profiles and Gravitational Behavior:** Figure **1** illustrates the radial evolution of energy density and pressure for several choices of the Rastall parameter. Both quantities achieve their maximum values at the stellar center and decrease monotonically towards the boundary, ensuring a physically coherent interior structure.

- **Quark Density Regularity and Positivity:** The distribution of quark matter displayed in Fig. **2** remains strictly positive throughout the configuration. This confirms the physical admissibility of the quark component and supports the suitability of the Durgapal-Fuloria ansatz for describing ultra-dense matter.

- **Influence of the Rastall Parameter on Stellar Composition:** Figure **3** depicts the impact of varying the Rastall parameter on the matter variables. The resulting profiles remain smooth, stable, and well-controlled, indicating that modifications introduced by $\mathcal{RT}$ do not compromise the physical regularity of the system.

- **Fulfillment of Classical Energy Conditions:** Figure **4** demonstrates that all standard energy conditions hold throughout the star. This verifies that the stellar matter is entirely non-exotic and adheres to the fundamental physical expectations for realistic compact objects.
- **Equation of State Behavior:** The variation of the EOS parameter ω^{Ras} presented in Fig. **5** consistently satisfies $0 < \omega^{Ras} < 1$. This confirms the presence of conventional, non-exotic matter within the ultra-dense environment of the star.
- **Mass, Compactness, and Redshift:** The mass function grows monotonically, the compactness factor remains below the Buchdahl limit $(2M/R < 8/9)$, and the redshift profile remains finite and well-behaved. These results collectively verify that the configuration satisfies all essential constraints imposed by general relativistic compactness bounds.
- **Causality and Adiabatic Stability:** Figure **6** confirmed that the stellar structure satisfies the causality condition $0 < v_s^2 < 1$ and obeys the adiabatic stability requirement for the considered values of Φ. These conditions demonstrate that the system remains dynamically stable under perturbations.

Furthermore, it is important to emphasize that the introduction of $\mathcal{RT}$ does not compromise the physical viability of the stellar configurations. While variations in the Rastall parameter modify the internal matter distribution. These changes are moderate and controlled. Specifically, as the Rastall parameter increases, the pressure and the energy density decrease, while the quark matter density ρ_q increases. Despite these variations, all matter variables maintain smooth radial profiles, positivity and adherence to classical energy conditions, while causality and stability criteria are satisfied throughout. The solutions also smoothly recover the general relativistic limit for $\Phi \to 0$, confirming the internal consistency of the model within $\mathcal{RT}$.

Overall, observations endorse that $\mathcal{RT}$ serves as a suitable and physically captivating framework for simulating ultra-dense star objects. The current model is singularity-free, realistic, dynamically stable, and complies with all main physical criteria. Thus, this study provides a thorough and physically credible description of compact stars impacted by changed gravitational dynamics, thereby setting the groundwork for future empirical and theoretical investigations. Meanwhile, the proposal's robustness naturally opens up avenues for further investigation, including modifications to rotating systems, anisotropic matter dynamics, alternative quark-matter EoS, and potential collisions with subsequent astrophysical or gravitational-wave observations.

Acknowledgment

We are grateful to the comments and suggestions of the referees which have contributed to improve this work.

References

[1] D. Barraco, V. H. Hamity, *Maximum mass of a spherically symmetric isotropic star*, Phys. Rev. D, **65** (2002), 124028. 4.4
[2] A. R. Bodmer, *Collapsed nuclei*, Phys. Rev. D, **4** (1971), 1601. 1
[3] H. A. Buchdahl, *General relativistic fluid spheres*, Phys. Rev., **116** (1959), 1027. 4.4, 4.4
[4] J. V. Cabrera, J. Estevez-Delgado, A. R. Romero, N. C. Muńoz, J. A. R. Ceballos, *An anisotropic stellar model in Rastall theory*, Mod. Phys. Lett. A, **40** (2025), 2550057. 1
[5] S. Chandrasekhar, *Dynamical instability of gaseous masses approaching the Schwarzschild limit*, Phys. Rev. Lett., **12** (1964), 114. 4.5
[6] S. Chandrasekhar, *The equilibrium and stability of the Darwin ellipsoids*, Astrophys. J., **140** (1964), 599–620. 4.5
[7] K. S. Cheng, Z. G. Dai, T. Lu, *Strange stars and related astrophysical phenomena*, Int. J. Mod. Phys. D, **7** (1998), 139–176. 1
[8] A. Chodos, R. L. Jaffe, K. Johnson, C. B. Thorn, V. Weisskopf, *New extended model of hadrons*, Phys. Rev. D, **9** (1974), 3471. 1

[9] F. Darabi, H. Moradpour, I. Licata, Y. Heydarzade, C. Corda, *Einstein and Rastall theories of gravitation in comparison*, Eur. Phys. J. C, **78** (2018), 25. 1

[10] K. P. Das, U. Debnath, M. Biswas, *Charged anisotropic strange stars in generalized Rastall gravity*, Phys. Scr., **100** (2025), 025305. 1

[11] M. C. Durgapal, R. S. Fuloria, *Analytic relativistic model for a superdense star*, Gen. Relativ. Gravit., **17** (1985), 671–681. 1, 3

[12] N. K. Glendenning, *Compact Stars: Nuclear Physics, Particle Physics and General Relativity*, Springer, New York, (2000), 322–323. 1

[13] M. K. Gokhroo, A. L. Mehra, *Anisotropic spheres with variable energy density in general relativity*, Gen. Relativ. Gravit., **26** (1994), 75–84. 1

[14] A. Golovnev, *More on the fact that Rastall = GR*, Ann. Phys., **461** (2024), 169580. 1

[15] S. Hansraj, A. Banerjee, *Dynamical behavior of the Tolman metrics in f(R,T) gravity*, Phys. Rev. D, **97** (2018), 104020. 1

[16] L. Herrera, *Cracking of self-gravitating compact objects*, Phys. Lett. A, **165** (1992), 206–210. 4.5

[17] N. Iqbal, S. Khan, M. Alshammari, W. W. Mohammed, M. Ilyas, *Nonmetricity-based hybrid self-gravitating compact stars with embedded class-one symmetry*, Eur. Phys. J. C, **85** (2025), 1–17. 1

[18] N. Itoh, *Hydrostatic equilibrium of hypothetical quark stars*, Prog. Theor. Phys., **44** (1970), 291–292. 1

[19] A. Malik, A. Shafaq, R. Manzoor, Z. Yousaf, A. Ali, *Stability analysis of anisotropic stellar structures in Rastall theory of gravity utilizing cracking technique*, Chin. J. Phys., **89** (2024), 613–627. 1

[20] G. Mustafa, X. Tie-Cheng, M. F. Shamir, *Self-consistent embedded anisotropic quintessence compact stars in Rastall gravity via linear equation of state*, Phys. Scr., **96** (2021), 105008. 1

[21] T. Naseer, *Role of Rastall gravity in constructing new spherically symmetric stellar solutions*, Phys. Dark Univ., **46** (2024), 101663. 1

[22] T. Naseer, *Complexity and isotropization based extended models in the context of electromagnetic field: an implication of minimal gravitational decoupling*, Eur. Phys. J. C, **84** (2024), 1256. 1

[23] T. Naseer, M. Sharif, *Role of decoupling and Rastall parameters on Krori–Barua and Tolman IV models*, Class. Quantum Grav., **41** (2024), 245006. 1

[24] G. Panotopoulos, A. Övgün, *Strange quark stars and condensate dark stars in Bumblebee gravity*, Nucl. Phys. B, **1017** (2025), 116956. 1

[25] F. Rahaman, P. K. F. Kuhfittig, R. Amin, G. Mandal, S. Ray, N. Islam, *Quark matter as dark matter in modeling galactic halo*, Phys. Lett. B, **714** (2012), 131–135. 1

[26] P. Rastall, *Generalization of the Einstein theory*, Phys. Rev. D, **6** (1972), 3357. 1, 2

[27] P. Rastall, *A theory of gravity*, Can. J. Phys., **54** (1976), 66–75. 1

[28] P. Rej, *Isotropic Durgapal IV fluid sphere in bigravity*, Can. J. Phys., **102** (2023), 100–112. 1

[29] P. Rej, *Charged analog of anisotropic dark energy star in Rastall gravity*, Int. J. Geom. Meth. Mod. Phys., **22** (2025), 2450329. 1

[30] P. Rej, P. Bhar, *Relativistic isotropic stellar model in f(R,T) gravity with Durgapal-IV metric*, New Astron., **105** (2024), 102113. 1, 4.5

[31] A. Saha, K. B. Goswami, P. K. Chattopadhyay, *Maximum mass and radius of higher-dimensional anisotropic strange quark star*, Int. J. Geom. Meth. Mod. Phys., **22** (2025), 2550107. 1

[32] M. Sallah, M. Sharif, *Impact of Charge on Strange Compact Stars in Rastall Theory*, Universe, **11** (2025), 25. 1

[33] S. Sarkar, D. Bhattacharjee, K. B. Goswami, P. K. Chattopadhyay, *New class of anisotropic charged strange quark star in Durgapal IV metric*, Astrophys. Space Sci., **369** (2024), 19. 1

[34] U. Sheikh, Y. Aziz, M. Z. Bhatti, R. Pincak, *On evolution of compact stars from string fluid in Rastall gravity*, Int. J. Geom. Meth. Mod. Phys., **20** (2023), 2350058. 1

[35] A. Singh, G. P. Singh, A. Pradhan, *Cosmic dynamics and qualitative study of Rastall model with spatial curvature*, Int. J. Mod. Phys. A, **37** (2022), 2250104. 1

[36] M. Sinha, S. S. Singh, *Strange Quark Stars with Kuchowicz Metric Function in Modified Gravitational Theory*, Int. J. Theor. Phys., **64** (2025), 197. 1

[37] H. Sohail, A. Ditta, I. Mahmood, S. K. Maurya, Y. M. Alanazi, *Rastall teleparallel gravity: gravitational decoupling with MGD approach*, Eur. Phys. J. Plus, **139** (8) (2024), 1–16. 1

[38] T. Tangphati, A. Banerjee, S. Hansraj, A. Pradhan, *The criteria of anisotropic quark star models in Rastall gravity*, Ann. Phys., **452** (2023), 169285. 1

[39] M. Visser, *Rastall gravity is equivalent to Einstein gravity*, Phys. Lett. B, **782** (2018), 83–86. 1

[40] A. Waseem, *Isotropic compact stars admitting Heintzmann solution in Rastall gravity*, Int. J. Geom. Meth. Mod. Phys., **21** (2024), 2450194. 1

[41] A. Waseem, *Tolman IV perfect fluid sphere in Rastall gravity*, Int. J. Geom. Meth. Mod. Phys., **21** (2024), 2450112. 1

[42] A. Waseem, T. Chaudhary, S. Naeem, B. Almutairi, F. Javed, *Insights on the stability of compact stars under Durgapal–Lake metric potentials*, Phys. Dark Univ., **46** (2024), 101609. 1

[43] A. Waseem, A. Eid, S. Naeem, F. Javed, *Impact of Rastall parameter on anisotropic stellar structures using Durgapal-Lake metrics and quintessence dark energy*, Nucl. Phys. B, (2025), 117068. 1

[44] A. Waseem, S. Naeem, *Study of isotropic stellar models via Durgapal-Lake solutions in Rastall system*, Phys. Scr., **99** (2024), 125023. 1

[45] E. Witten, *Cosmic separation of phases*, Phys. Rev. D, **30** (1984), 272. 1